J-PARC Letter of Intent: Search for a Permanent Muon Electric Dipole Moment at the $10^{-24}\,\mathrm{e}\cdot\mathrm{cm}$ Level.

A. Silenko, **Belarusian State University, Belarus**

R.M. Carey, V. Logashenko, K.R. Lynch, J.P. Miller*, B.L. Roberts

Boston University

G. Bennett, D.M. Lazarus, L.B. Leipuner, W. Marciano,

W. Meng, W.M. Morse, R. Prigl, Y.K. Semertzidis*

Brookhaven National Lab

V. Balakin, A. Bazhan, A. Dudnikov, B. Khazin, I.B. Khriplovich, G. Sylvestrov

BINP, Novosibirsk

Y. Orlov, **Cornell University**

K. Jungmann, **Kernfysisch Versneller Instituut, Groningen**

P.T. Debevec, D.W. Hertzog, C.J.G. Onderwater, C. Ozben

University of Illinois

E. Stephenson, **Indiana University**

M. Auzinsh, **University of Latvia**

P. Cushman, Ron McNabb, **University of Minnesota**

N. Shafer-Ray, **University of Oklahoma**

K. Yoshimura, **KEK, Japan**

M. Aoki, Y. Kuno#, A. Sato, **Osaka, Japan**

M. Iwasaki, **RIKEN, Japan**

F.J.M. Farley, V.W. Hughes, **Yale University**

January 9, 2003

* Spokesperson, # Resident Spokesperson

1 Abstract

The baryon-antibaryon asymmetry in the universe requires CP violating phases in addition to the one present in the CKM matrix of the Standard Model (SM). Electric dipole moments (EDM) of elementary particles naturally provide information on these additional phases. The EDM values predicted by the SM are several orders below the current experimental sensitivities and hence the observation of any EDM would be an unmistakable indication of new physics. We propose to use the large polarized muon flux anticipated to be available from J-PARC to search for a muon EDM at the $10^{-24}\,\mathrm{e}\cdot\mathrm{cm}$ level with systematic errors well below that. At that level, and for a CP violating phase of order 1, the muon EDM experiment will be a factor of 100 more sensitive to new physics than is probed by the current muon g-2 experiment. The experimental design exploits the strong motional electric field sensed by relativistic particles in a magnetic storage ring.

Contents

2 Introduction

A non-zero measurement of the muon electric dipole moment (EDM) is unmistakable evidence of physics beyond the Standard Model. Unlike the magnetic dipole moment, the existence of a permanent EDM in a muon (or any other elementary particle) violates time reversal and parity symmetries, with the Standard Model predicted value for the muon being well below the $10^{-24}\,\mathrm{e}\cdot\mathrm{cm}$ sensitivity of our proposed measurement. A measurement at this level would be at least 5 orders of magnitude more precise than the current measurements, and would be sensitive to a host of proposed models of physics beyond the Standard Model.

The J-PARC facility will provide the perfect setting for such an ambitious measurement. With the addition of a muon decay line and pulsed-beam capability, the PRISM beamline proposed for J-PARC will be the only beamline capable of providing the flux necessary for our statistical error within a one-year running period. However, the demanding systematic error budget will require a two stage development of the experiment. In the first stage, we will measure the EDM of the deuteron. Deuterons can be produced copiously and a measurement of its EDM is more sensitive to the known systematic errors. In the second stage, building on our work in stage one, we will make a measurement of the muon EDM. Both the muon and deuteron measurements will take place in the same storage ring and both will use the novel technique of combining $\vec{E}$ and $\vec{B}$ fields to minimize all non-EDM induced spin precessions.

Equipment for stage one will be developed at Brookhaven National Laboratory. Our goal will be to set a new experimental limit on the deuteron EDM, currently estimated [2, 3] to be $< 4 \times 10^{-25}\,\mathrm{e}\cdot\mathrm{cm}$ based on neutron and mercury EDM measurements. After the Brookhaven EDM measurements are complete, the storage ring and the deuteron source will be moved to a muon beamline for the muon EDM measurement. We will alternate deuteron and muon injection in the PRISM beamline, in order to control systematic errors.

We are preparing a proposal to US funding agencies to develop the deuteron and muon experiments. We estimate the cost to be about \$10-\$15 million (U.S.). Once funding is in place, it will take about four years to construct the storage ring and detectors, and to complete the first phase, namely the measurements of the deuteron EDM. We note that the participation of BNL personnel would require the concurrence of the U.S. Department of Energy.

3 Motivation

The Standard Model of particle physics provides a successful theoretical framework for describing all known particles and their interactions. However, the Standard Model also leaves many fundamental questions unanswered. Among the least understood phenomena is CP violation. At present, the only known source of CP violation in the Standard Model is a phase in the CKM matrix. Its fundamental origins are unknown. Further, while CP violation is an essential ingredient of almost all attempts to explain the matter-antimatter asymmetry of the universe [4],[1] the amount of CP violation present in the CKM matrix is insufficient to explain the observed asymmetry [6, 7, 8, 9]. Searches for CP violation beyond the CKM matrix are necessary to shed light on this puzzle and are also probes of physics beyond the Standard Model.

Electric dipole moments (EDMs) of elementary particles violate both parity (P) and time reversal (T) invariance. If CPT is assumed to be a valid unbroken symmetry, a permanent EDM is, then, a signature of CP violation [10, 11]. A non-vanishing permanent EDM has not been measured for any elementary particle. In the Standard Model, EDMs are generated only at the multi-loop level and are predicted to be many orders of magnitude below the sensitivity of foreseeable experiments [12, 13]. A non-vanishing EDM measurement therefore would be unambiguous evidence for CP violation beyond the CKM matrix, and searches for permanent EDMs of fundamental particles are powerful probes of extensions of the Standard Model.

The muon anomalous magnetic moment, a_μ, and electric dipole moment, d_μ, can be related to each other [14, 15, 16] as the real and imaginary parts of a more general dipole moment, D. The interaction of the electromagnetic field tensor, $F_{\mu\nu}$, with the general dipole operator is given by

$$\mathcal{L}_{\mathrm{DM}} = \frac{1}{2}\left[D\bar{\mu}\sigma^{\alpha\beta}\frac{1+\gamma_5}{2} + D^*\bar{\mu}\sigma^{\alpha\beta}\frac{1-\gamma_5}{2}\right]\mu\, F_{\alpha\beta} \tag{1}$$

where $\sigma^{\alpha\beta} = \frac{1}{2}\left[\gamma^\alpha, \gamma^\beta\right]$ and

$$a_\mu \frac{e}{2m_\mu} = \Re D \tag{2}$$

$$d_\mu = \Im D, \tag{3}$$

[1] Alternative explanations are subject to stringent bounds. See, e.g., Ref. [5].

where $\Re D$ and $\Im D$ are correspondingly the real and imaginary parts of D. Writing $D^{NP} = |D^{NP}|\, e^{i\phi_{\rm CP}}$ as the contribution of "New Physics" to D provides a measure of the relative probing power of a_μ and d_μ experiments. If "New Physics" gives rise to a discrepancy between experiment and Standard Model expectations, $a_\mu^{\rm NP} = a_\mu^{\rm exp} - a_\mu^{\rm SM}$, then one expects that same "New Physics" to induce a muon EDM given by

$$d_\mu^{\rm NP} \simeq 3 \times 10^{-22} \left(\frac{a_\mu^{\rm NP}}{3 \times 10^{-9}} \right) \tan\phi_{\rm CP} \ \ {\rm e} \cdot {\rm cm}\ . \tag{4}$$

Of course, the values of $a_\mu^{\rm NP}$ and $\tan\phi_{\rm CP}$ are model dependent.

For the current situation (assuming the e^+e^- data for the hadronic contribution) [17, 18, 19]

$$a_\mu^{\rm exp} - a_\mu^{\rm SM} \simeq 3(1) \times 10^{-9} \tag{5}$$

one expects

$$d_\mu^{\rm NP} \simeq 3 \times 10^{-22} \ \tan\phi_{\rm CP} \ \ {\rm e} \cdot {\rm cm}\ . \tag{6}$$

So, exploring down to $d_\mu \sim 10^{-24}\,{\rm e} \cdot {\rm cm}$ would probe

$$\tan\phi_{\rm CP} \geq 3(1) \times 10^{-3}. \tag{7}$$

as shown in Fig. (1) [16].

Even if no deviation in $a_\mu^{\rm exp} - a_\mu^{\rm SM}$ were discovered and new physics were constrained to $|a_\mu^{\rm NP}| \leq 1 \times 10^{-9}$, a measurement or bound on d_μ at $10^{-24}\,{\rm e} \cdot {\rm cm}$ would push the combined constraint on $a_\mu^{\rm NP} \tan\phi_{\rm CP}$ to

$$|a_\mu^{\rm NP} \tan\phi_{\rm CP}| \leq 10^{-11} \tag{8}$$

i.e. 100 times the probing power for $\tan\phi_{\rm CP}$ of order 1.

What value of $\tan\phi_{\rm CP}$ can be expected in realistic extensions of the Standard Model? Supersymmetric models which easily accommodate $a_\mu^{\rm NP} \sim 3 \times 10^{-9}$ via one loop gaugino-slepton contributions can have fairly arbitrary $\tan\phi_{\rm CP}$ phases. In some models, a symmetry may lead to very small $\tan\phi_{\rm CP}$ expectations. In those cases, a bound of $10^{-24}\,{\rm e} \cdot {\rm cm}$ combined with a measurement of $a_\mu^{\rm NP} \sim 3 \times 10^{-9}$ would lead to the significant constraint

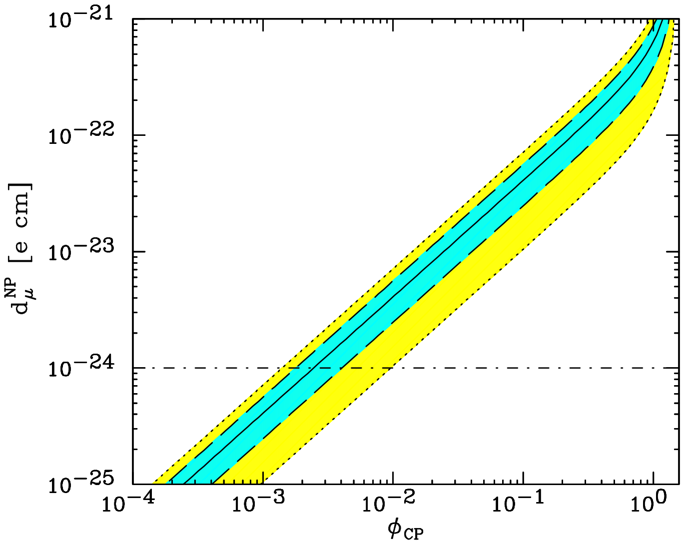

Figure 1: Regions of the $(\phi_{\rm CP}, d_\mu^{\rm NP})$ plane suggested by the current E821 data at the 1σ and 2σ [16]. The horizontal line shows the experimental sensitivity of the muon EDM at J-PARC to $d_\mu^{\rm NP}$.

$$|\tan\phi_{\rm CP}| \leq 0.003. \tag{9}$$

Alternatively, if no symmetry suppresses the value of $\tan\phi_{\rm CP}$, one might expect $\tan\phi_{\rm CP}$ to be of order 1 and a muon EDM of

$$d_\mu^{\rm NP} \simeq 3\times 10^{-22}\,{\rm e}\cdot{\rm cm}\ . \tag{10}$$

With 10^{-24} e $\cdot$ cm precision, the combination $a_\mu^{\rm NP}\tan\phi_{\rm CP}$ would be determined to about $\pm 0.3\%$, a remarkable feat. That would open a window to a new type of CP violation, one with significant strength that might be related to the baryon-antibaryon asymmetry of our universe.

Within specific models, predictions for the muon EDM vary widely [20, 21, 22, 23, 24]. In particular, the left-right supersymmetric model with the seesaw mechanism of reference [25] predicts d_μ as large as 5×10^{-23} e $\cdot$ cm, 50 times larger than the sensitivity of the proposed experiment. The prediction for the EDM of the electron is of order 10^{-28} e $\cdot$ cm, 10 times smaller than the present experimental limit [26].

Sensitive EDM searches are presently being carried out on neutral objects, i.e. neutrons, atoms and molecules. This choice was strongly influenced by the Ramsey-Purcell-Schiff theorem [27] which states that for point-like charged objects in electromagnetic equilibrium the net electric field averages to zero. The widely known loopholes so far were weak and strong nuclear forces, weak electron-nucleon forces and relativistic forces. It is recognized now that this theorem is also not applicable to particles in a storage ring, particularly to the method proposed here, where motional fields are employed, because it is not possible to factorize particle velocity and electric field, which constituted the basis of the theorem [27, 28]. Therefore these electric fields, which are very strong for relativistic particles, can be beneficially exploited. Such fields can be three orders of magnitude higher than technically achievable fields between electrodes.

If an EDM were observed in another system, a measurement of the muon EDM would be complementary and of extreme importance in understanding the nature of the effect [29].

4 Concept of Experiment

In the presence of both electric and magnetic fields, oriented orthogonally to the muon velocity and to each other, the angular frequency of muon spin precession relative to the momentum is given by

$$\vec{\omega} = -\frac{e}{m}\left\{a\vec{B} + \left(\frac{1}{\gamma^2-1} - a\right)\frac{\vec{\beta}\times\vec{E}}{c} + \frac{\eta}{2}\left(\frac{\vec{E}}{c} + \vec{\beta}\times\vec{B}\right)\right\}, \tag{11}$$

where $a = (g-2)/2$ and η is the EDM in units of $\frac{e\hbar}{4mc}$.

The magnetic and electric dipole moments are given by $\mu = \frac{g}{2}\frac{e\hbar}{2m}$ and $d = \frac{\eta}{2}\frac{e\hbar}{2mc}$, respectively. η plays a role for the EDM corresponding to the g factor for the magnetic dipole moment. The muon EDM couples to the external fields through the $\eta(\vec{E} + c\vec{\beta}\times\vec{B})$ term. The external B-field couples to the EDM because it produces an E-field in the rest frame of the muon. In fact, for the parameters envisioned in the present proposal, the motional E-field from the $\vec{\beta}\times\vec{B}$ term is far larger than that due to the applied E-field. The EDM value is given in terms of the dimensionless parameter η by

$$d_\mu = \frac{\eta}{2}\frac{e\hbar}{2m_\mu c} \simeq \eta \times 4.7\times10^{-14}\ \mathrm{e\cdot cm}. \tag{12}$$

for the muon.

Assuming that the EDM is 0, from Eq. (11), it is clear that at the "magic" γ, ($\gamma = 29.3$)

$$\frac{1}{\gamma^2-1} - a = 0, \tag{13}$$

and the muon spin precession depends only on g-2 and the average B-field. The anomalous precession frequency, due to the *magnetic* moment, is measured by observing the time spectrum of muon decay electrons. In the muon rest frame, the highest energy electrons are emitted preferentially along the muon spin vector. As the spin vector precesses relative to the momentum vector, the number of high energy electrons observed in the lab frame is modulated at the precession frequency.

However, the experimental technique used to measure a_μ, which is the one used by the $g-2$ experiment at BNL, may not be well suited for a simultaneous measurement of the EDM. From Eq. (11) (at the muon "magic" momentum) it is apparent that the EDM influence on the spin precession is two-fold

1. The spin precesses about an axis which is not exactly parallel to the magnetic field but is tipped from the vertical in the radial direction by an angle $\delta = \tan^{-1} \frac{\eta\beta}{2a}$. The plane of precession is thus rotated out of the plane of the storage ring.

2. The spin precession frequency is increased by a factor of $\sqrt{(1+\delta^2)}$.

Both of the above effects were exploited in the last CERN muon g-2 experiment to set a limit on the EDM [31]. In method 1, they searched for an up down asymmetry in the positron counting rate using a detector split on the vertical mid-plane. The presence of an EDM would induce an oscillating difference between the counting rate of the two parts of the detector. The frequency of that difference signal would be ω_a, with an amplitude proportional to the EDM. The reported limit is $3.7 \pm 3.4 \times 10^{-19}\,\mathrm{e\cdot cm}$. The error is the combined result of the statistical and systematic errors, which were about equal in magnitude:

- Statistical: $\pm 2.7 \times 10^{-19}\,\mathrm{e\cdot cm}$
- Systematic: $\pm 2 \times 10^{-19}\,\mathrm{e\cdot cm}$

In method 2, any difference between the expected value of a_μ and that measured is attributed to a non-zero EDM and the result was consistent, with comparable errors. E821 plans to use method 1 to determine d_μ with statistical and systematic errors $\approx 1 \times 10^{-19}\,\mathrm{e\cdot cm}$.

Neither of the two methods is adequate beyond $10^{-19}\,\mathrm{e\cdot cm}$ precision. In method 2, no attempt is made to separate the two effects of the magnetic and electric dipole moments.

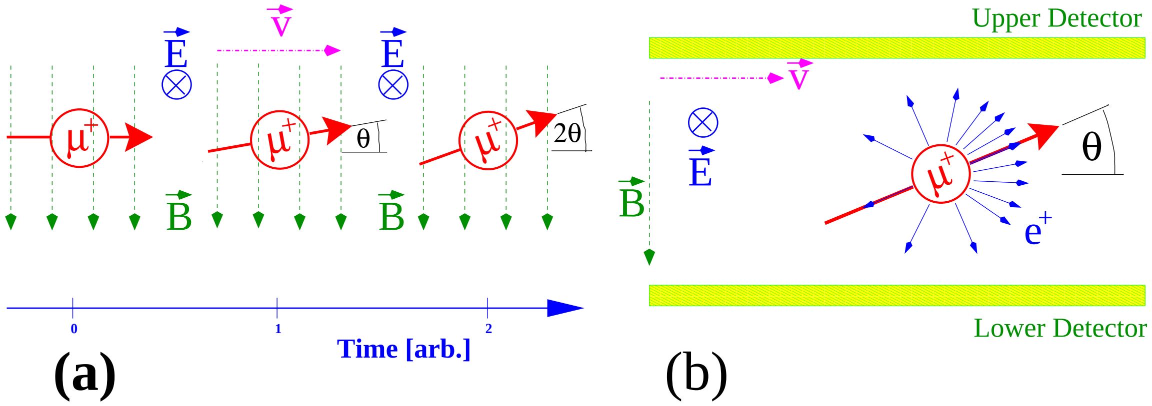

Figure 2: The basic principle of the proposed experiment. (a) Relativistic muons (μ^+) of velocity $\vec{v}$ moving in a magnetic storage ring with field ($\vec{B}$) are exposed to a motional electric field $\vec{E} \propto \vec{v} \times \vec{B}$. In case of a finite small EDM the muon spin precesses with a linear increase in precession angle θ in time about an axis which is directed radially. (b) Due to the spatial anisotropy in the decay $\mu^+ \to e^+ + \nu_e + \overline{\nu_\mu}$ detectors above and below the storage region are expected to observe a time dependent change in the ratio of positron counting signals. The positron angular distribution is indicated by the density of arrows.

Method 1 is inherently plagued by systematic errors because the EDM signal sits at the same frequency as that produced by the magnetic dipole moment. Indeed, the effect of a (presumably small) EDM is *obscured* by the anomalous precession. Any wobbling of the spin precession plane produced by an EDM at one moment in the precession period is canceled half a period later, when the spin's radial and azimuthal coordinates have been reversed.

For the dedicated EDM experiment proposed in this document we will follow a new approach:

1. Use muons with much lower energies, and

2. employ a radial electric field which cancels the g-2 precession.

The electric field in the lab required to cancel the g-2 precession is

$$E \simeq aBc\beta\gamma^2, \tag{14}$$

which we will conservatively [32] assume to be technically limited to about 2 MV/m. Using Eqs. (11, 14) the spin precession angular frequency is given by:

$$\vec{\omega} = -\frac{e}{m}\frac{\eta}{2}\left(\frac{\vec{E}}{c} + \vec{\beta}\times\vec{B}\right), \tag{15}$$

i.e. the g-2 precession is canceled and only the EDM is left to act on the spin. The torque in the center of mass is given by

$$d\vec{S}/dt' = \vec{d}\times\vec{E}'. \tag{16}$$

which in terms of laboratory quantities is

$$d\vec{S}/dt = \vec{d}\times(\vec{E} + c\vec{\beta}\times\vec{B}). \tag{17}$$

As previously mentioned, for realizable values for the applied E-field, the "motional" E-field from the $\vec{\beta}\times\vec{B}$ term is much larger than that from the $\vec{E}$ term.

Thus the muon spin direction will be "frozen" relative to the muon momentum if the EDM is zero. In the presence of a non-zero EDM, the radial E-field in the muon's rest frame will cause rotation of the spin in a vertical plane about an axis parallel to the radial direction. As the spin acquires a vertical component, the decay positron momenta also acquire a vertical component, resulting in an up-down asymmetry in the number, $R_N = \frac{N_{up}-N_{down}}{N_{up}+N_{down}}$ (or average energy, $R_E = \frac{E_{up}-E_{down}}{E_{up}+E_{down}}$) of electrons or positrons which *grows linearly with time*, see Figs. (2,3). Together with other improvements, which will significantly reduce many systematic errors, this new experimental approach will improve our sensitivity to a muon EDM by five orders of magnitude.

5 PRISM-II Muon Beam Line

The search for the muon EDM at a sensitivity of $10^{-24}\mathrm{e}\cdot\mathrm{cm}$ requires a high intensity polarized muon beam capable of obtaining $NP^2 = 10^{16}$, where N and P are the number of muons and their polarization respectively. Such a highly intense polarized muon beam can only be achieved by the novel scheme of PRISM at an accelerator such as J-PARC. PRISM consists of

1. Pion capture by using a high-field solenoid magnet system (pion capture section).

2. Semi-adiabatic transfer of the captured pions to a lower solenoid field (matching section).

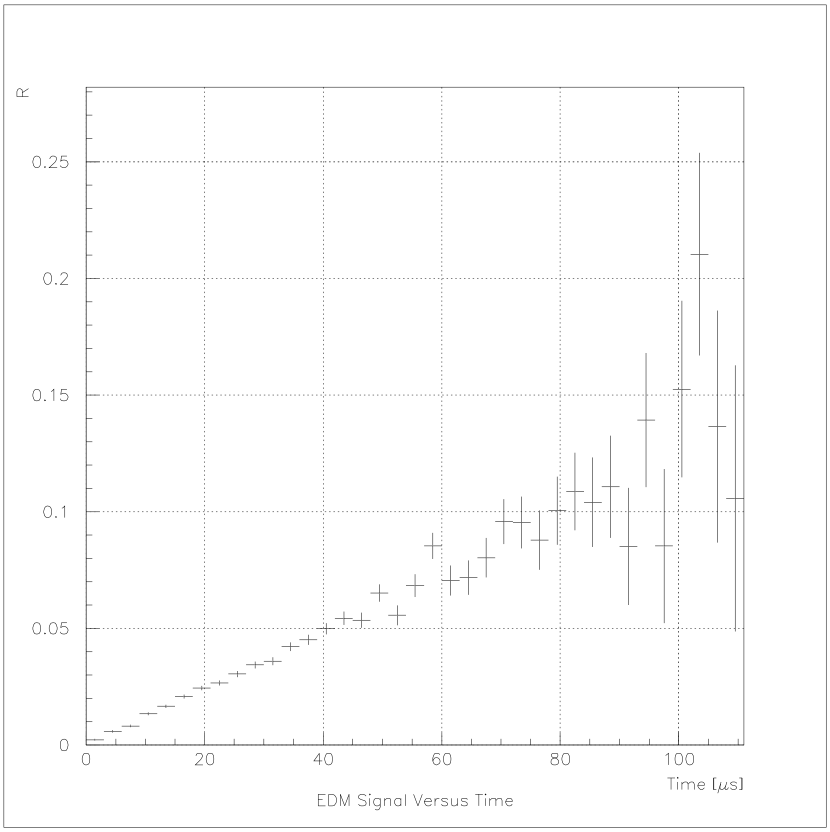

Figure 3: MC simulation of the muon EDM signal, $R = \frac{N_{up}-N_{down}}{N_{up}+N_{down}}$, versus time.

3. Selection of the pion momentum (curved solenoid section).

4. Decay of pions to muons (pion decay and muon transport section).

5. Selection of the muon momentum, and

6. Compression of the muon momentum spread by using fixed field alternating gradient (FFAG) phase rotator.

Since the momentum acceptance of the muon storage EDM ring would be limited to a level of $\Delta p/p \simeq 2\%$, it is desirable to employ the phase rotation technique to reduce the energy spread with minimum loss of muons. By using phase rotation, the momentum spread of the muon beam can be reduced by more than an order of magnitude, from $\Delta p/p = \pm 30\%$ to $\Delta p/p \simeq \pm 2\%$. This would provide a sufficient number of polarized muons injected into the muon storage EDM ring.

To accomplish a phase rotated muon beam for the EDM experiment, a new beam facility has to be constructed. We refer to it as PRISM-II. The major difference from PRISM-I (which is primarily for the $\mu^- - e^-$ conversion experiment) is in the momentum range of the muon beam, namely 68 ± 17 MeV/c for PRISM-I and 0.5 ± 0.15 GeV/c for PRISM-II. The design of PRISM-II consists of three major components; (1) construction of a new FFAG phase rotator for 0.5 GeV/c muons, (2) installation of curved solenoids to select the pion momentum to improve the muon polarization, (3) installation of a longer pion decay solenoid. Regarding the target and the pion capture solenoid, it has been found that the same designs as those in PRISM-I can be used.

5.1 Pion Capture at Forward Take-off Angle

Table (1) summarizes the current design parameters of PRISM-II except for the FFAG phase rotator. The design parameters for the FFAG phase rotator are shown in Table (2). The requirement for the muons injected into the PRISM-II FFAG is to provide polarized muons with momentum range of 350 MeV/c $< P_\mu <$ 650 MeV/c with NP^2 as large as reasonably achievable, where N is the number of the muons available to the experiment and P is the muon polarization.

Fig. (4) shows the results of a Monte-Carlo simulation of the longitudinal muon polarization as a function of initial pion momentum, where pions corresponding to muon momenta of 350 MeV/c $< P_\mu <$ 650 MeV/c are shown. The corresponding pion momenta are 350 MeV/c $< P_\pi <$ 1.1 GeV/c. Fig. (4) shows that backward-decay muons have a rather higher polarization than forward-decay muons. By selecting pions with $P_\pi > 0.7$ GeV/c, NP^2 is maximized and pion contamination of the muon beam is avoided.

The field strength of superconducting solenoid magnets in the present technology would be 12 T or more. However, if a potential heat load to the magnet due to high neutron flux coming from the production target is considered, it would be conservative to start considering a lower field strength such as 6 T. Thus, a 6 T-superconducting solenoid magnet for the pion collection magnet is assumed in the present design. Fig. (5) shows the P_T distribution of the initial pions for a muon beam emittance of 800 π mm·mrad for both the horizontal and vertical phase spaces, and muon momenta of 350 MeV/c $< P_\mu <$ 650 MeV/c. The inner bore could be the same as in PRISM-I, 10 cm at 6 T, so that initial pions of $P_T <$ 100 MeV/c can be accepted and the muon yields are not significantly degraded, Fig. (5).

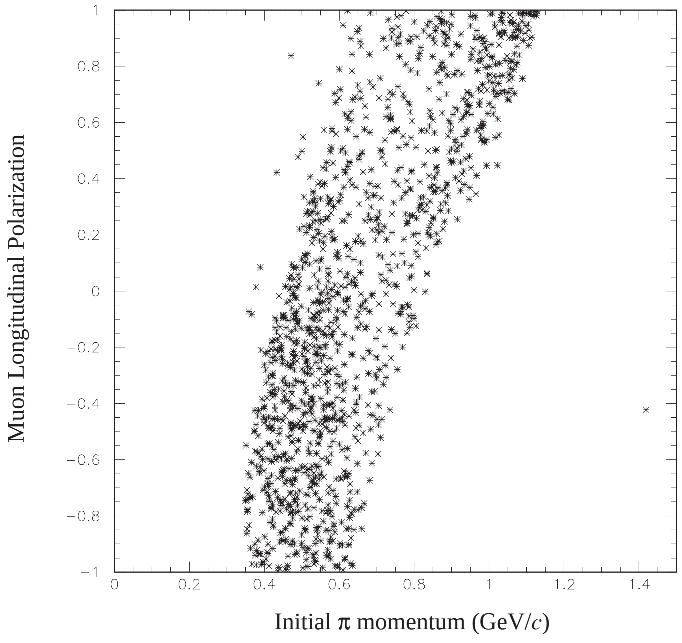

Figure 4: Muon longitudinal polarization versus initial pion momentum. Muons are selected with horizontal and vertical acceptances 800 π mm·mrad each and momentum acceptance 350 MeV/$c < p_\mu <$ 650 MeV/c.

5.2 Pion Decay and Muon Transport Solenoid

The pions collected by the capture solenoid are transfered to the pion decay and muon transport solenoid, in which the pions decay in flight into muons. Since the momentum range of the initial pions are around 1 GeV/c, and its $\tau\beta\gamma c$ is almost 80 m, the decay solenoid should be at least 80 m long. However, it would be difficult to accommodate an 80 m solenoid magnet in the experimental hall. Therefore, a solenoid magnet of 20 m long is considered in the present design with about 25% of the pions decaying into muons. If it is possible to find room for a longer transport solenoid, the muon yield would be greater.

If the high magnetic fields in the pion capture section and the low magnetic field of the pion decay section can be connected without any magnetic field leakage and the field gradient is sufficiently small, the charged particles through the channel will be transferred adiabatically. In adiabatic transfer, B/p_t^2 and BR^2 are preserved, where B is the magnetic field strength, p_t is the transverse momentum and R is the radius of the helix of the charged particle. Thus, Rp_t is independent of the field strength in adiabatic transfer. On

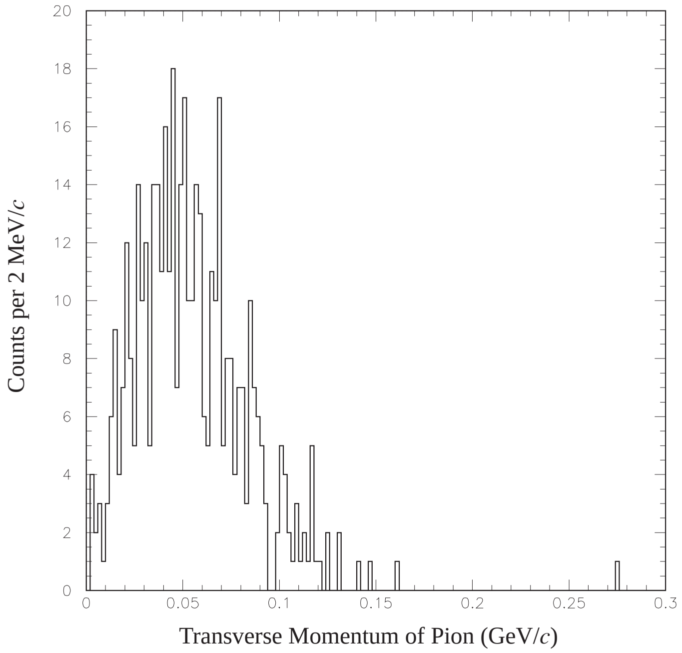

Figure 5: Transverse momenta of pions from a production target with daughter muons being selected with horizontal and vertical acceptance of the muon storage ring, 800 π mm·mrad, and momentum acceptance 350 MeV/c $< p_\mu <$ 650 MeV/c at the exit of the decay solenoid.

the other hand, the muon yield into a fixed acceptance at the exit of the decay solenoid scales linearly with $1/R^2p_t^2$ of the beam. As a result, the muon yield is almost independent of the magnetic field strength of the decay solenoid as long as the adiabatic transfer is maintained. This increases the freedom of design, and the field strength of the decay solenoid could be much lower than that of the capture solenoid. We chose 1T as the field strength of the decay solenoid for the current design.

The transfer between the capture solenoid and the decay solenoid is actually not perfect for 1 GeV/c pions since the pitch of the helix of the pion trajectory is several meters for this momentum region. If the length of the matching section was 20 m or more, perfectly adiabatic transfer could be restored for 1 GeV/c pions at the cost of an expensive solenoid magnet system. We performed Monte Carlo simulations and estimated the phase space of pions after the matching section, and found that the 4.5 m length of the matching solenoid of the current design results in pion distributions similar to adiabatic transfer. Although not an adiabatic transfer, the choice of the length of the matching solenoid happens to match the pitch of helix for 1 GeV/c pions.

The expected size of pion beam after 4.5 m of the matching section is $R_D = 10$ cm $\times \sqrt{6 \text{ T}/1 \text{ T}} \simeq 25$ cm. Muons may have transverse momenta up to 30 MeV/c from pion decay, which results in an increase of the beam size by at most 20 cm. The radius of the decay solenoid is chosen to be about 45 cm so that the muons from pion decay would be safely contained without hitting the inner bore.

5.3 Selection of Pion Momentum to Improve Muon Polarization

The pion momenta selection could be achieved by using a curved solenoid. This technique is also being adopted in the MECO (BNL-E940) experiment. In a curved solenoid, charged particles follow helical trajectories with a drift in the direction perpendicular to the plane of the curved solenoid. The distance of the drift (D) after traversing a length s in the torus is given by

$$D = \frac{1}{0.3B} \times \frac{s}{R} \times (p_s^2 + \frac{1}{2}p_t^2)/p_s \,,$$

where R is the curvature of the solenoid, and p_t and p_s are the perpendicular and parallel momentum components, respectively. The drift can be further controlled by applying an additional magnetic field, called a compensation field, perpendicular to the plane of the curve; the net drift of the particle with the particular p_t and p_s could be thus adjusted to zero.

Fig. (6) shows a momentum spectrum of the charged particles at the exit of a 50°-curved solenoid, when particles are distributed uniformly in the momentum range 0 – 2.0 GeV/c at the entrance of the solenoid. The torus field is 1 T, the compensation magnetic field is 0.60 T, the inner bore radius of the torus is 45 cm, and the radius of curvature is 5 m in the present calculation. A transmission efficiency of almost 90% can easily be achieved by selecting pions with momenta $P_\pi > 0.7$ GeV/c. The momentum spread of the transmitted particles and the position of the transmission window can be easily adjusted by changing the length of the arc and the compensation field, respectively.

It is worth mentioning here that the current design is not a unique solution to the muon beam line for the muon EDM experiment. The pion capture, semi-adiabatic transition, and curved solenoid could be replaced with a horn magnet system. Further optimization studies will be made.

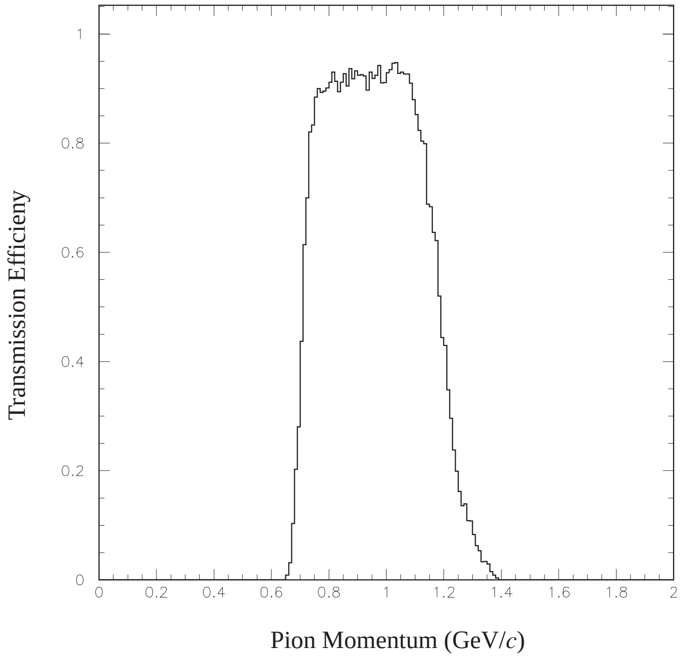

Figure 6: The transmission probability of charged particles as a function of momentum for the curved solenoid, where the field strength at the center of solenoid is 1 T, the major radius of the curved solenoid is 5 m, the minor radius of the curved solenoid is 45 cm, and the degree of curve is 50°.

6 PRISM-II FFAG

A preliminary design of the PRISM-II FFAG ring has been made. The PRISM-II FFAG accelerator can be either a normal conducting magnet FFAG or a superconducting one. The main difference is the bending strength and the average radius; 1.8 T and 21 m, respectively, for the normal conducting and 2.8 T and 10 m for the superconducting version, respectively. Figs. (7) and (8) show a schematic of the normal conducting version and its lattice functions in one sector and those for superconducting one, respectively. Table (2) summarizes the main parameters of the PRISM-II FFAG ring. The normal conducting version has to have more cells, twice as many, although the length of each cell is about the same for both versions, that is 4 m, resulting in the similar maximum value of the beta functions. The dispersion function of the superconducting version is 50% greater than that of the normal one. The superconducting FFAG can be accommodated in the initially proposed area of the experimental hall.

It should be noted that the design of the PRISM-II FFAG ring is the same as the first FFAG ring of the Japanese Neutrino Factory. The first ring would accelerate muons from 0.3 GeV/c to 1.0 GeV/c. The PRISM-II FFAG ring would serve an important role towards the realization of a neutrino factory in Japan.

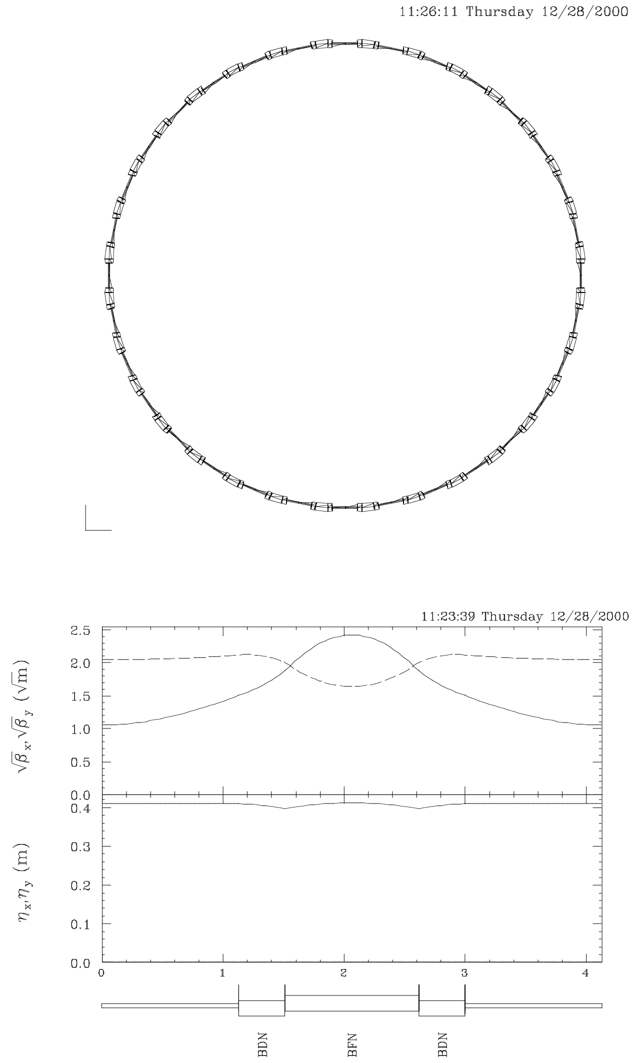

Figure 7: Normal conducting version of the PRISM-II FFAG ring. The average radius of the ring is 21 m.

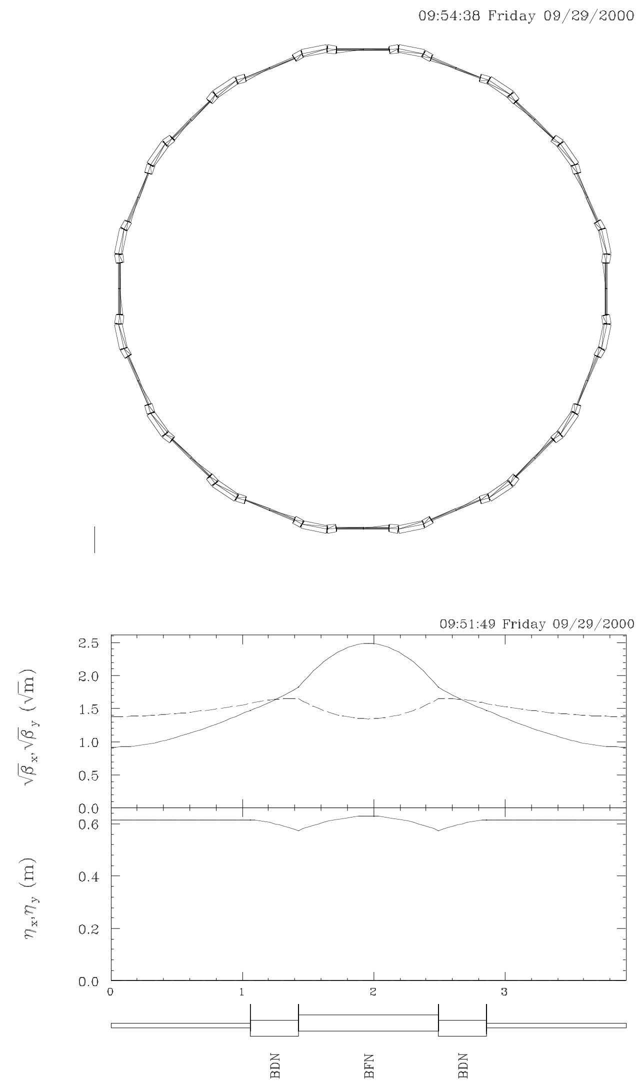

Figure 8: Superconducting version of the PRISM-II FFAG ring. The average radius of the ring is 10 m.

6.1 Estimation of Muon Yield and Muon Polarization

Monte Carlo simulations using GEANT 3.21+FLUKA were performed to estimate the muon yield and muon polarization. The Monte Carlo simulations were made from pion production to the exit of the muon transport solenoid. The original GEANT 3.21 code was modified so that it could handle transport of the muon polarization in a magnetic field.

RF acceleration of muons in the PRISM-II FFAG phase rotator would be at a level of 1 MeV/m. Thus, muons of 750 MeV/c should travel through the ring for almost 150 m to get decelerated down to 500 MeV/c. The length of 150 m corresponds to only 2.5 turns in the superconducting FFAG phase rotator (even if the packing factor of the RF cavities is not long). Muon depolarization due to the $g-2$ precession would be thus negligible. The decay loss of the muons in the FFAG phase rotator would be several percent. A tracking study in the PRISM-II FFAG ring with computer aided simulation is being undertaken.

Table (3) summarizes the expected muon yield and polarization. The estimated NP^2 is about 5×10^{16} for the muon momentum being 500 MeV/c. The NP^2 was also estimated for the lower muon momentum option such as 350 MeV/c, and is about 3×10^{16}. Both cases are sufficient for our goal.

7 Storage Ring Lattice

The EDM ring lattice must meet the following requirements: Firstly, in order to minimize systematic errors, the g-2 precession must be canceled, according to Eq. (14), not merely on average over the ring, but with some accuracy, at every point where the magnetic field rotates the muon magnetic moment. This condition means that the cylindrical electric plates should be placed between the magnetic poles. For better accuracy of cancellation, the magnetic field in such places should be homogeneous; therefore, the beam-focusing quadrupoles should be placed outside of the dipole magnetic and electric fields.

Secondly, to minimize systematic errors, we will alternately inject clockwise (CW) and counterclockwise (CC) into the muon storage ring. The polarity of the magnetic dipole field is changed, while the electric and quadrupole fields stay the same. In both polarities, the dipole magnetic field will be adjusted to cancel the g-2 precession.

Finally, there is the requirement to have free spaces between lattice elements for experimental devices such as the deuteron polarimeters and calorimeters to detect electrons

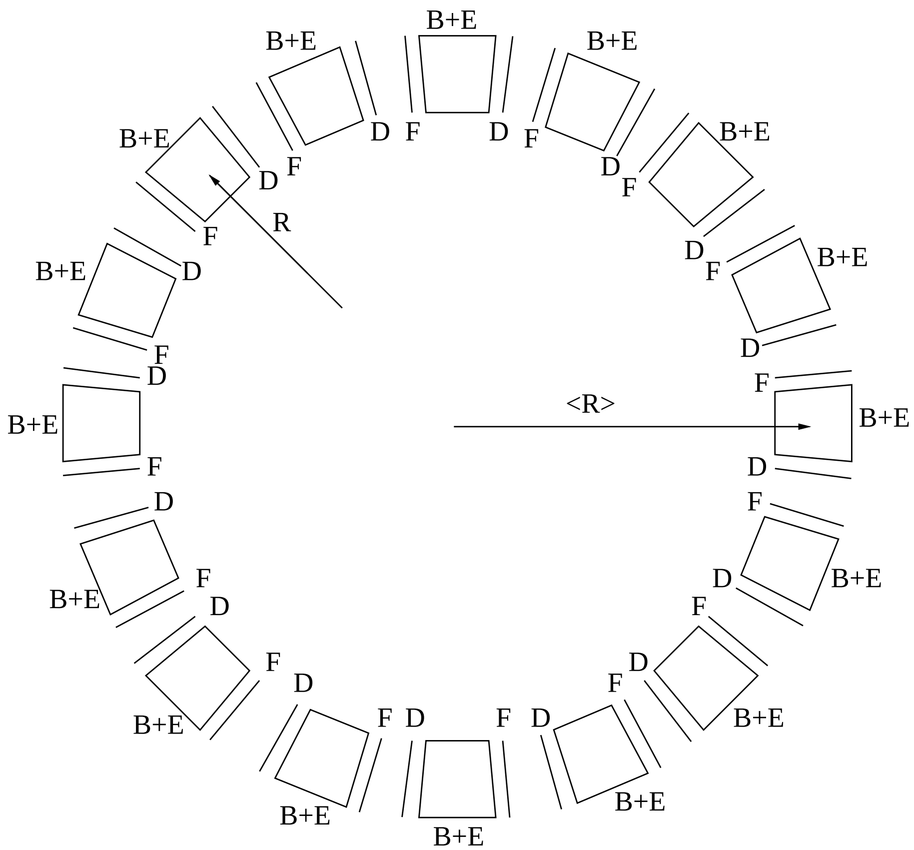

Figure 9: A schematic of the lattice (not to scale) of the EDM ring for the 0.5 GeV/c momentum case. $R \approx 6.5$ m, while the average radius around the ring, including regions with no dipole magnetic field, is $< R > \approx 11$ m.

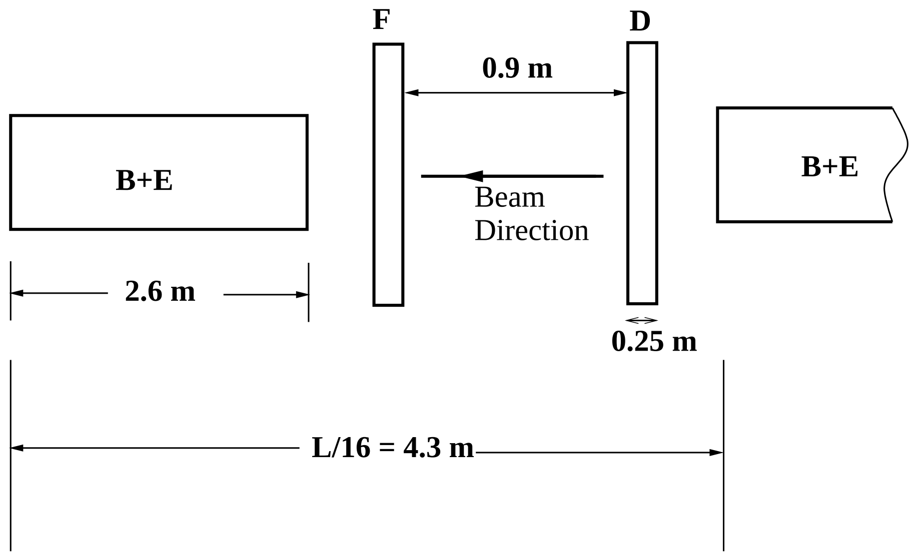

Figure 10: One period of the EDM ring lattice. The ring contains 16 such periods. The strength of the focusing (F) and de-focusing (D) quadrupoles is the same.

from muon decay, and devices for beam manipulations (like kickers). We are optimizing the choice of beam momentum, which we currently estimate to be in the range of 0.3-0.5 GeV/c. Lower momentum would have the advantage of needing less space. We present here, Figs. (9, 10), a solution for $P \approx 0.5$ GeV/c. The intervals between B+E sections have been chosen to be 1.7 m long with the B+E sections 2.6 m long. In every interval we symmetrically place one focusing and one defocusing lens, with a free space about 0.9 m between them. To minimize undesirable spin perturbations, the lattice is maximally symmetrical, with 16 small periods each containing one B+E section, one free interval and two lenses each. Under the assumption of Eq. (14), with E at the practical limit of E=2 MV/m, the magnetic field $B \approx 0.25$ T. The corresponding radius of curvature in the regions with dipole magnetic field is $R \approx 6.5$ m, while the average radius around the ring, including regions with no dipole magnetic field, is $< R > \approx 10$ m. Since our lenses can be rather short, say, 25 cm, there will be about 15 m of integral free space for the needed experimental and beam/spin manipulating devices. In this ring, the betatron tunes are $\nu_x \sim 4.42$ and $\nu_y \sim 4.2$ and the maximal values of the corresponding β-functions are $\beta_{x\,max} = 6.85$ m and $\beta_{y\,max} = 7.1$ m. The storage ring aperture will be optimized to match the emittance of the beam of 800 π mm mrad. As an example, we can rather easily get horizontal and vertical admittances of $\sim 1.4 \times 10^3\,\pi$ mm mrad with momentum acceptance of $\Delta P/P \sim 2\%$ by using an aperture of 20 cm $\times$ 20 cm.

8 Possible Experimental Area Layout

A possible layout of the pulsed proton beam facility consists of the near facility (closer to the 50-GeV PS) and the far facility (beyond the public road). The PRISM-II and the EDM ring will be installed in the near facility.

A close-look layout of the near facility is shown in Fig. (11). The hall is composed of two areas. In one of them, PRISM-II (for a 300/500 MeV/c muon beam) is installed with about 20 m long pion decay section, together with PRISM. In the other area, the EDM ring can be placed.

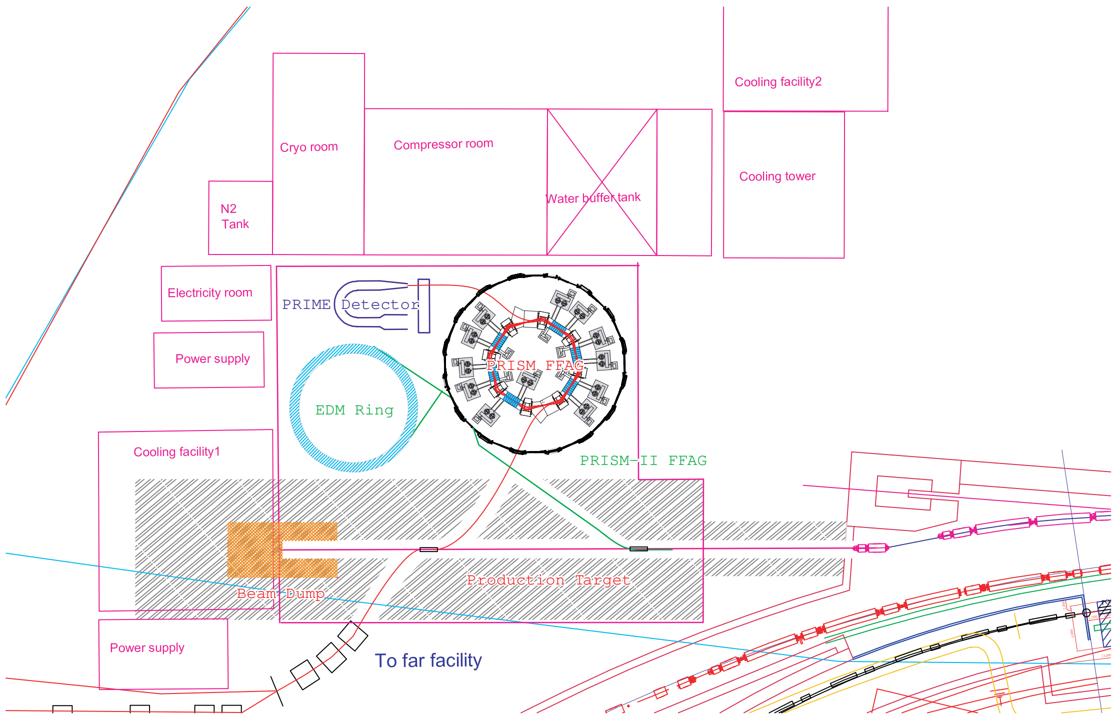

Figure 11: A possible layout of the near facility where PRISM and PRISM-II are installed.

The pulsed proton beam facility, including a primary proton beam line, a production target, and a beam dump, must be constructed by J-PARC. It is hoped that the PRISM-II ring and the pion decay section consisting of a 20 m long superconducting solenoid magnet will be provided by J-PARC, although we will do their design work and will try to obtain funding for them to some extent in Japan.

9 Detectors

We require a detector system which is sensitive to the changes in distribution of muon decay electrons/positrons going upward compared to the number going downward, in an energy range of 100 to 500 MeV. Electron detectors will be placed above and below the muon storage region. Instantaneous rates will be high, therefore we will integrate the energy deposited as a function of time, rather than measure the time and energy of each electron or positron. The muon EDM is proportional to the rate of change with time of the ratio $R_E = \frac{E_{up}-E_{down}}{E_{up}+E_{down}}$, where E_{up} and E_{down} are the energies in the up and down counters.

10 Systematic Errors

The difference between the cyclotron and spin precession frequencies is:

$$\vec{\omega} = -\frac{e}{m}\left[a\vec{B} + \left(\frac{1}{\gamma^2-1} - a\right)\frac{\vec{\beta}\times\vec{E}}{c} + \frac{\eta}{2}\left(\frac{\vec{E}}{c} + \vec{\beta}\times\vec{B}\right)\right]. \tag{18}$$

as discussed above. In the present experiment, a radial electric field is applied such that:

$$a\vec{B} + \left(\frac{1}{\gamma^2-1} - a\right)\frac{\vec{\beta}\times\vec{E}}{c} \approx 0. \tag{19}$$

Systematic effects from spin dynamics which rotate the spin into the vertical plane and thereby mimic the effect of the EDM, occur when the E field vectors are not in a plane around the ring. The same happens when the muon orbit, defined mostly by the B field, is not in a plane. Our main guard against the non-planar (NP) systematic effects is to inject the beam into the ring both clockwise (CW) and counterclockwise (CC). All non-planar E and B systematic effects we have studied with the present lattice have opposite relative sign compared to the EDM when injecting clockwise and counter-clockwise, and thus can in principle be canceled. We plan to alternate CW and CC on successive J-PARC cycles, ~ 0.5 Hz. The detector systematic errors, e.g. rate effects, are also largely canceled by injecting CW and CC.

It would be useful for spin dynamics systematic studies to find and use a particle species which can be produced more readily than muons with large polarization, and which, for a given ring size and B-field, has a similar electric field value $E \simeq aBcp\gamma/m$ as for the muon, i.e. a similar value for

$$f \equiv a\gamma/m$$

In Table (4) we give this factor for the muon, proton and deuteron for $p \simeq 0.5\,\mathrm{GeV/c}$. Although the muon and deuteron a, m and γ differ significantly, $f \equiv a\gamma/m$ is similar in magnitude. The deuteron is an excellent choice to use for systematic studies, since the storage of muons and deuterons, with the spin precession halted, could use almost the same values for the E- and B-fields.

A net non-planar electric field component, $E_{NP} = \theta_{NP}E$ will rotate the spin in the vertical plane by:

$$dS/dt = \mu\theta_{NP}E/\left(c\beta\gamma^2\right) \tag{20}$$

This is our most serious potential source of a false EDM signal. For the deuteron, $\mu = 0.857e\hbar/(2m_p)$, and for the muon, $\mu = 1.001e\hbar/(2m_\mu)$. For $p = 0.5$ GeV/c and $\theta E = 10^{-8} \times 2\mathrm{MV/m}$, $\omega_s = -28\,\mathrm{mrad/s}$ for the deuteron, and 2.3 mrad/s for the muon, i.e. this systematic effect is twelve times greater for the deuteron than for the muon.

The spin precession due to the EDM is:

$$d\vec{S}/dt = \vec{d} \times \left(\vec{E} + \vec{v} \times \vec{B}\right) \approx \vec{d} \times \left(c\vec{\beta} \times \vec{B}\right) \tag{21}$$

β is less for the deuteron compared to the muon, giving reduced sensitivity to the deuteron EDM, d_D. From the present limits on the EDM of the neutron, $d_n < 6 \times 10^{-26}\,\mathrm{e\cdot cm}$, and atomic mercury, $d_{Hg} < 10^{-27}\,\mathrm{e\cdot cm}$, Khriplovich [2, 3] deduced an indirect limit on the EDM of the deuteron: $d_D < 4 \times 10^{-25}\,\mathrm{e\cdot cm}$. Since we plan to use the deuteron to study spin dynamic systematic effects, this limit is adequate for a search for the muon EDM to the level of $\simeq 10^{-24}\,\mathrm{e\cdot cm}$. We are presently studying whether we can set a sensitive direct limit on the EDM of the deuteron. One complication is that the deuteron has an electric quadrupole moment of $Q = 2.86 \times 10^{-27}\,\mathrm{e\cdot cm^2}$. However, $\vec{Q} \cdot \vec{\nabla} \times \vec{E}$ is small compared to $\vec{d} \cdot \vec{E}$ for our geometry. The deuteron beam emittance will be smaller than the muon beam emittance, so the deuteron beam will have to paint the storage ring admittance over different injections. We plan to take deuteron data between J-PARC cycles, as well as before and after the muon runs. Table (5) shows the different configurations we plan with the relative sign for the experimental observable for both the EDM and non-planar (NP) effects.

To summarize, the spin dynamic systematic effects will be canceled by injecting both clockwise and counter-clockwise. The spin dynamics systematic effects we have studied are larger for the deuteron than for the muon. We will study and minimize the systematic effects with deuterons. We discuss the deuteron polarimetry issues in the appendix.

11 Summary

We propose to search for an EDM of the muon in a dedicated storage ring at the level of $10^{-24}\,\mathrm{e}\cdot\mathrm{cm}$. Since the Standard Model prediction is far smaller, the measurement of a non-zero EDM is a direct indication of new physics. Indeed, a number of supersymmetric models predict a muon EDM significantly larger than our proposed sensitivity. Under the assumption of CPT invariance, a non-zero muon EDM violates CP symmetry, and indicates the presence of a new source of CP violation, perhaps shedding light to the baryon-antibaryon asymmetry of the universe. If the CP violating phase is of order one, then the measurement will be 100 times more sensitive to new physics than the current measurement of the muon anomalous magnetic moment.

In storage ring measurements, one can exploit the electric field in the muon rest frame which results from the laboratory magnetic field. This so-called motional E-field, can be far larger than any practical applied E-field, which greatly increases the sensitivity of the measurement. However, the sensitivity of our proposed measurement, a 5 orders of magnitude improvement over the anticipated result from the muon $g-2$ experiment, will require a radically new technique. Muons, with $p \approx 0.5\,\mathrm{GeV/c}$, will be stored in a strong-focusing ring. The $\vec{E}$ and $\vec{B}$ fields in the ring will be chosen so that the Larmor and Thomas precessions sum to zero relative to the momentum precession, leaving only that due to an EDM. The result is a large amplification of the EDM signal, unobscured by other spin motions.

Vertical spin precession arising from radial B-fields or vertical E-fields, which can mimic an EDM signal, will largely cancel when muons are injected in both the clockwise and counter-clockwise directions. Residual errors can be studied by storing polarized deuterons on alternate pulses, for which the needed $\vec{E}$ and $\vec{B}$ fields are fortuitously close to those of the muon. The deuteron turns out to be more sensitive to systematic errors associated with, for example, imperfections in the field distributions, but has less precession due to its own EDM, and is therefore ideally suited for systematic studies.

Our proposed systematic error will require that the experiment be developed in two phases. In the first phase, we will develop a storage ring at Brookhaven National Laboratory for the deuteron EDM measurement. Perfecting the ring for the deuteron measurement is, apart from the detector system, equivalent to perfecting it for the muon EDM measurement. In the second phase, the storage ring will be moved to a high-flux pulsed muon source for the muon EDM measurement. J-PARC is the only funded facility in the world which can provide the large, high energy pulsed proton flux that is required along with a high repetition rate. Finally, the proposed high flux PRISM II muon source, also unique in the world, should produce sufficient numbers of polarized muons for us to reach our proposed sensitivity in a one-year run.

12 Appendix

12.1 Deuteron Polarimetry

This appendix describes some of the considerations needed for a measurement of the direction and magnitude of the polarization of a deuteron test beam circulating in the ring used for the EDM experiment. Features that will reduce systematic errors in the measurements are noted.

A beam from a polarized source has an axis of quantization determined by the orientation of the magnetic field at the point where the atomic deuterium is converted into either a bare nucleus or the negative ion, D^-. Along this axis, a vector polarization can be created by increasing the population of either the $m = 1$ or $m = -1$ magnetic substates relative to the other. (Depopulation of the $m = 0$ substate can make more deuterons available to increase the vector polarization at the expense of also introducing a tensor polarization. This is not a major problem and will not be addressed here.) From atomic beam sources [33], one can obtain polarizations, $p = f_1 - f_{-1}$, f_i being the fractional occupation of a substate, of about 0.9. The sign of the polarization can be flipped using RF-transition units that connect specific hyperfine states in atomic deuterium, a feature that is extremely helpful in reducing systematic errors in any test of the spin characteristics of the ring.

Information about the magnitude and direction of the deuteron polarization is available by observing the spin-dependence in the scattering cross section from some target that intercepts the circulating beam. Since the strong interaction is parity-conserving, the component of the polarization that lies along the momentum direction is not accessible [2]. The two transverse components will each produce an azimuthal asymmetry on either side of the plane that contains that component and the beam direction. For the y-component, this is:

$$\sigma(\theta, \phi) = \sigma_0(\theta)\ [1 + (3pA(\theta)/2)\ \cos\phi] \tag{22}$$

where ϕ begins along the $\hat{x}$ direction and $A(\theta)$ is the vector analyzing power, a property of the specific nuclear reaction taking place. Detectors placed to the left and right (where symmetry will again help to reduce systematic errors) around the cosine maxima will observe different cross sections. The asymmetry $\epsilon = 3pA/2$ is obtained from $(L-R)/(L+R)$, where L and R are the respective counting rates. If one combines such a two-detector system with measurements from both positively and negatively polarized deuteron beams, then the extraction of ϵ from

$$\epsilon = 3pA/2 = \frac{(r-1)}{(r+1)}, \qquad \text{where} \qquad r^2 = \frac{L(+)R(-)]}{[L(-)R(+)]} \tag{23}$$

will cancel any error arising from a spin-independent difference between the detector efficiencies or the amount of positively or negatively polarized beam that circulates.

Deuteron test beams will have momenta of about 400 MeV/c (or kinetic energy near 40 MeV). At these energies, there is much information available in the literature on the vector analyzing power $A(\theta)$ from various targets. Both hydrogen and carbon have analyzing powers that are large in useful ranges of scattering angle and targets can be constructed from hydrocarbon materials. One possible polarimeter design would detect deuterons elastically scattered from carbon at laboratory angles between 27° and 40°. Over that range, the average $\langle 3A/2 \rangle = -0.43$ with an azimuthally integrated cross section of 16 mb [34]. Elastic collisions with hydrogen produce two easily detected products, the proton and deuteron. If deuterons at laboratory angles between 19° and 27° are observed in coincidence with protons between 40° and 60°, the data will have an average analyzing power of $\langle 3A/2 \rangle = -0.38$ with an integrated cross section of 38 mb [35]. The scattered deuterons and protons from these elastic processes are easily detected using plastic scintillators that

[2] Interference with the weak interaction does produce effects at the level of 10^{-7}.

have the advantage of quick response and excellent time resolution. If an azimuthal array of such counters is segmented four ways to produce a left-right pair and an up-down pair, then both the x and y components of the deuteron polarization would be available. A check for consistency between the carbon and hydrogen target results would be helpful. All of the laboratory angles are in a single hemisphere. So from a single target, identical arrays of detectors mounted fore and aft would make it possible to obtain measurements for deuterons circulating in either direction in the ring.

The counting rate goes as $C = N_T N_B \sigma \Omega$ where N_T is the areal density of the target, N_B is the beam flux in particles/s, σ is the cross section, and Ω is the solid angle subtended by the detectors. If C is the sum of the rates over all detectors and beam spin directions, then the error in the asymmetry goes as

$$\delta\epsilon = \delta(3pA/2) = \frac{1}{\sqrt{C}} \tag{24}$$

It is expected that the EDM will produce polarization components that increase steadily with time. Testing this with deuteron beams will require that the asymmetries from different times in the store will be compared. Looking for *changes* will help to reduce any systematic errors that would shift small components away from zero, such as a small rotational misalignment that would tend to mix x and y components in the detectors.

12.2 Inclinometer

To monitor the mechanical stability of the EDM ring we are developing inclinometers with high sensitivity. At present we are developing a differential capacitor inclinometer which has a pendulum center electrode, with the outer electrodes fixed to the surface to be measured. The position of the central electrode is thus determined by the local gravitational field. Readout is by means of a bridge circuit. Proven sensitivity to date is greater than 200 nanoradians/volt providing better than 1 nrad relative sensitivity. The device is small, enclosed in a micro-environment $\sim 10\,\mathrm{cm} \times 10\,\mathrm{cm} \times 3\,\mathrm{cm}$. Dynamic range is about 3 milliradians.

The next phase of development will focus on long term stability and sensitivity to changes in temperature, pressure, and other external conditions.

References

[1] "AGS Letter of Intent-Search for a Permanent Muon Electric Dipole Moment", submitted to BNL, February 11, 2000. The manuscript is also available from http : //www.bnl.gov/edm/papers/loiedm0002_v3.ps.

[2] I. B. Khriplovich, "Nuclear Electric Dipole Moments at Ion Storage Rings," Workshop Proceedings on Nuclear Electric Dipole Moment Searches, GSI, Darmstadt, Germany, Nov 9-10, 1999, pp. 1-24.

[3] I. B. Khriplovich, and R. V. Korkin, "P and T odd electromagnetic moments of deuteron in chiral limit," Nucl. Phys. **A665**, 365 (1999).

[4] A. D. Sakharov, "Violation Of CP Invariance, C Asymmetry, And Baryon Asymmetry Of The Universe," Pisma Zh. Eksp. Teor. Fiz. **5**, 32 (1967) [JETP Lett. **5**, 24 (1967)].

[5] A. G. Cohen, A. De Rujula and S. L. Glashow, "A matter-antimatter universe?," Astrophys. J. **495**, 539 (1998) [astro-ph/9707087].

[6] G. R. Farrar and M. E. Shaposhnikov, "Baryon asymmetry of the universe in the standard electroweak theory," Phys. Rev. D **50**, 774 (1994) [hep-ph/9305275].

[7] M. B. Gavela, P. Hernandez, J. Orloff and O. Pene, "Standard Model CP violation and baryon asymmetry," Mod. Phys. Lett. A **9**, 795 (1994) [hep-ph/9312215].

[8] M. B. Gavela, P. Hernandez, J. Orloff, O. Pene and C. Quimbay, "Standard Model CP violation and baryon asymmetry. Part 2: Finite temperature," Nucl. Phys. B **430**, 382 (1994) [hep-ph/9406289].

[9] P. Huet and E. Sather, "Electroweak baryogenesis and Standard Model CP violation," Phys. Rev. D **51**, 379 (1995) [hep-ph/9404302].

[10] S. M. Barr and W. J. Marciano, "Electric Dipole Moments," BNL-41939, in "CP Violation", ed. C. Jarlskog, World Scientific, Singapore (1989)

[11] W. Bernreuther and M. Suzuki, "The electric dipole moment of the electron," Rev. Mod. Phys. **63**, 313 (1991) [Erratum-ibid. **64**, 633 (1991)].

[12] F. Hoogeveen, "The Standard Model Prediction for the Electric Dipole Moment of the Electron," Nucl. Phys. B **341**, 322 (1990).

[13] I. B. Khriplovich, "Quark Electric Dipole Moment And Induced Theta Term In The Kobayashi-Maskawa Model," Phys. Lett. B **173**, 193 (1986) [Sov. J. Nucl. Phys. **44**, 659.1986 YAFIA,44,1019 (1986)].

[14] W. Marciano, HIMUS99 Workshop, Tsukuba (1999).

[15] M. Graesser and S. Thomas, "Supersymmetric relations among electromagnetic dipole operators," hep-ph/0104254.

[16] J. L. Feng, K. T. Matchev and Y. Shadmi, "Theoretical expectations for the muon's electric dipole moment," hep-ph/0107182.

[17] G. W. Bennett *et al.* [Muon g-2 Collaboration], "Measurement of the positive muon anomalous magnetic moment to 0.7 ppm," Phys. Rev. Lett. **89**, 101804 (2002) [hep-ex/0208001].

[18] M. Davier et al., hep-ph/0208177.

[19] K. Hagiwara, A. D. Martin, D. Nomura, T. Teubner, hep-ph/0209187.

[20] A. Pilaftsis, Nucl. Phys. **B644**, 263 (2002).

[21] K.S. Babu, B. Dutta, and R.N. Mohapatra, Phys. Rev. Lett. **85**, 5064 (2000).

[22] J.L. Feng, K.T. Matchev, and Yael Shadmi, Nucl. Phys. **B613**, 366 (2001).

[23] J.R. Ellis et al., Phys. Lett. **B528** 86 (2002).

[24] A. Romanino and A. Strumia, Nucl. Phys. **B622**, 73 (2002).

[25] K. S. Babu, B. Dutta and R. N. Mohapatra, "Enhanced electric dipole moment of the muon in the presence of large neutrino mixing," Phys. Rev. Lett. **85**, 5064 (2000) [hep-ph/0006329].

[26] B.C. Regan *et al.,* "New Limit on the Electron Electric Dipole Moment", Phys. Rev. Lett. **88**, 071805 (2002).

[27] L.I. Schiff, Phys.Rev. **132**, 2194 (1963).

[28] P.G.H. Sandars, Workshop on Nuclear electric Dipole Moment Searches, GSI, Darmstadt (1999).

[29] K. S. Babu, C. Kolda, J. March-Russell and F. Wilczek, "CP violation, Higgs couplings, and supersymmetry," Phys. Rev. D **59**, 016004 (1999) [hep-ph/9804355].

[30] F.J.M. Farley and E. Picasso, "Quantum Electrodynamics", ed. by T. Kinoshita (World Scientific, Singapore, 1990), p. 479.

[31] J. Bailey, K. Borer, F. Combley, H. Drumm, F.J.M. Farley, J.H. Field, W. Flegel, P.M. Hatterley, F. Krienen, F. Lange, E. Picasso, and W. von Rüden, J. Phys. **G4**, 345 (1978); J. Bailey *et al.*, Nucl. Phys. **B150**, 1 (1979).

[32] A. Yamamoto, A. Maki, A. Kusumegi, Nucl. Instrum. Methods **148**, 203 (1978).

[33] W. Haeberli, Ann. Rev. of Nucl. Sci. **17**, 373 (1967).

[34] S. Kato *et al.*, Nucl. Instrum. Methods **A238**, 453 (1985).

[35] K. Hatanaka *et al.*, Nucl. Phys. **A325**, 205 (1984); see also H. Witała *et al.*, Few-Body Systems **15**, 67 (1993).

Table 1: The design parameters of PRISM-II, not including the FFAG section.

Production Target	
Material	Graphite
Length	80 cm
Diameter	2.0 cm
Superconducting Pion Capture Solenoid	
Magnetic Field Strength	6 T
Length	120 cm
Inner Bore Radius	10 cm (inside the radiation shield)
Transverse Momentum Acceptance	< 100 MeV/c
Material of the radiation shield	Tungsten
Thickness of the radiation shield	30 cm
Maximum heat load to the cold coil	less than 500 W
Superconducting Matching Solenoid	
Magnetic Field Strength	6 T – 1 T
Length	450 cm
Inner Bore Radius	10 cm – 45 cm
Transverse Momentum Reduction Factor	$\simeq 40\%$
Superconducting Torus Solenoid	
Magnetic Field Strength	1 T (at the center of bore)
Compensation Field Strength	0.60 T
Major Radius	5 m
Inner Bore Radius	45 cm
Angle of Arc	50°
Transmission Efficiency	90% for 0.7 – 1.1 GeV/c
Sharpness of the Cut-off	80 MeV/c (10–90%)
Superconducting Decay Solenoid	
Magnetic Field Strength	1 T
Inner Bore Radius	45 cm
Length	20 m
Fraction of Pion Decays	25%

Table 2: Main parameters of PRISM-II FFAG.

Parameters	normal conducting	super-conducting
number of sector	32	16
k value	50	15
transition gamma	7.1	4
orbit excursion	0.50 m	0.77 m
average radius	21 m	10 m
B@F/D	1.8 T	2.8 T
F/2 angle	0.026 rad	0.052 rad
D angle	0.018 rad	0.036 rad
F/2 bend angle	17 degree	26 degree
packing f	0.45	0.46
phase advance(H/V)	120/61 deg.	131/103 deg.
drift length	2.060 m	2.120 m
BF length	1.104 m	1.065 m
BD length	0.382 m	0.367 m

Table 3: The expected muon yield and NP^2 for the PRISM-II

Muon Momentum	500 MeV/c	350 MeV/c
Momentum Acceptance of the FFAG ring	$\pm 30\%$	$\pm 30\%$
Horizontal and Vertical Acceptance of the muon EDM ring	800 π mm·mrad	800π mm·mrad
Yield of Unpolarized Muon per proton (50 GeV/c)	0.040%	0.025%
Yield of Polarized Muon per proton (50 GeV/c)	0.016%	0.009%
Muon Polarization (Longitudinal)	60%	64%
Expected NP^2 per 10^7 seconds at J-PARC	5×10^{16}	3×10^{16}

Table 4: The factor f for different particles.

Particle	S	a	$(1+p^2/m^2)^{1/2}$	m (MeV/c^2)	f
μ	1/2	0.001166	≈ 5	105	0.054
p	1/2	1.793	≈ 1	938	1.912
d	1	-0.143	≈ 1	1876	-0.076

Table 5: Relative sign of B, E and the spin observable due to the EDM and from non-planar fields for muons and deuterons when injecting CW and CC. Both longitudinal (L) and radial (R) polarizations are possible with the deuteron.

Mode	B-field direction	E-field direction	EDM	E_{NP}, etc.
μ^+ CW	up	in	$+d_\mu$	$+E_{NP}$
μ^+ CC	down	in	$-d_\mu$	$+E_{NP}$
μ^- CW	down	out	$+d_\mu$	$+E_{NP}$
μ^- CC	up	out	$-d_\mu$	$+E_{NP}$
D_L CW	up	out	$+d_d/5$	$+12E_{NP}$
D_L CC	down	out	$-d_d/5$	$+12E_{NP}$
D_R CW	up	out	0	0
D_R CC	down	out	0	0